

Selected results on Strong and Coulomb-induced correlations from the STAR experiment

M. Šumbera* for the STAR Collaboration

Nuclear Physics Institute, Academy of Sciences of the Czech Republic, 250 68 Řež, Czech Republic

Using recent high-statistics STAR data from Au+Au and Cu+Cu collisions at full RHIC energy I discuss strong and Coulomb-induced final state interaction effects on identical ($\pi - \pi$) and non-identical ($\pi - \Xi$) particle correlations. Analysis of $\pi - \Xi$ correlations reveals the strong and Coulomb-induced FSI effects allowing for the first time to estimate space extension of π and Ξ sources and average shift between them. Source imaging technique providing clean separation of these effects from effects due to the source function itself is applied to one-dimensional relative momentum correlation function of identical pions. For low momentum pions and/or non-central collisions large departure from a single-Gaussian shape is observed.

Keywords: heavy ions,femtoscopy

I. INTRODUCTION

Progress in understanding space-time structure of multiparticle production via femtoscopy technique is currently driven by high-statistics data sets accumulated in heavy ion experiments at RHIC and SPS accelerators [1, 2, 3, 4, 10]. In particular ambitious program of the STAR collaboration at RHIC exploiting good particle identification has already provided vast variety of femtoscopy measurements in different identical and non-identical particle systems some of which were actually measured for the first time [4]. This contribution is a progress report on two currently pursued STAR femtoscopy analyses. Both of them were introduced already at the previous WPCF meeting last year in Kroměříž [2]. First focuses on non-identical particle correlations in rather exotic meson-baryon system $\pi^\pm - \Xi^\pm$ [5]. Previous investigations have shown that correlations among these two charged hadrons reveal not only the Coulomb but also the strong final state interaction (FSI) effects [11, 12]. Order of magnitude difference in mass plus $\Delta B=1/\Delta S=2$ gap in baryon/ strangeness quantum numbers makes $\pi - \Xi$ system an important tool to study the interplay between matter flow of on partonic and hadronic level. The second analysis exploits particle correlations in a more conventional system of two identical charged pions [6]. Its aim is to understand the geometry of the source. Ultimate and rather ambitious aspiration of this project is to extract pion-pion scattering lengths. This goal, not reached so far, will make heavy ion femtoscopy measurements fully competitive to a dedicated particle physics experiments trying to extract this important parameter of the strong interactions [3, 7, 8]. Basic prerequisites for such measurements are good knowledge of correlations due to quantum statistics and Coulomb interactions.

II. STUDYING SPACE-TIME STRUCTURE OF MULTI-STRANGE BARYON SOURCE VIA $\pi - \Xi$ CORRELATIONS

In ultra-relativistic heavy-ion collisions at RHIC hot and dense strongly interacting matter is created exhibiting prop-

erties of de-confined partonic matter [9, 13]. Almost instantaneous equilibration of produced matter indicated by recent heavy flavor measurements [9, 14] represent one of the greatest puzzles coming from the RHIC [9]. The early partonic collectivity also shows up in a subsequent evolution of the system leading to strong collective expansion of the bulk matter as demonstrated by large values of observed elliptic flow [9, 13]. These observations are further substantiated by STAR multi-strange baryon measurements showing that Ξ and Ω baryons reveal significant amount of elliptic flow which is comparable to ordinary non-strange baryons [15]. The sizable multi-strange baryon elliptic flow which obeys constituent quark scaling [16] confirms that substantial part of the collective motion has indeed developed prior to hadronization. This picture is also corroborated by more recent STAR analysis of the centrality dependence of hyperon yields carried out within the framework of a thermal model [17]. Observed scaling behavior of strange baryons is consistent with a scenario of hadron formation from constituent quark degrees of freedom through quark recombination provided that the coalescence took place over a volume that is much larger than the one created in any elementary collisions.

These observations fit nicely into ideal hydro evolution starting from the system of de-confined QCD matter. However they are also consistent with more realistic hybrid macroscopic/microscopic transport approach [20] which takes into account the strength of dissipative effects prevalent in the latter hadronic phase of the reaction. The hybrid model calculations indicate that at top RHIC energy the hadronic phase of the heavy-ion reaction is of significant duration (at least 10 fm/c) making hadronic freeze-out a continuous process, strongly depending on hadron flavor and momenta. In particular heavy hadrons, which are quite sensitive to radial flow effects, obtain the additional collective push created by resonant (quasi)elastic interactions during that fairly long-lived hadronic rescattering stage [21].

It is clear that question concerning multi-strange baryon decoupling from hot and strongly interacting partonic/hadronic system is an interesting one but also not an easy one to solve. Could this be provided by the femtoscopy? What kind of relevant information can be obtained via low-relative-velocity correlations of multi-strange baryons with the other hadrons? Since non-identical particle correlations are sensitive not only to the extent of the source, but also

*e-mail: sumbera@ujf.cas.cz

to the average shift in emission time and position among different particle species [19] the answer is affirmative. The femtoscopy of non-identical particles was already used to show that the average emission points of pions, kaons and protons produced in heavy-ion collisions at SPS and RHIC are not the same [3, 7, 10, 22, 23]. In hydrodynamically inspired blast-wave approach [18] mass ordering of average space-time emission points of different particle species naturally appears due to the transverse expansion of the source. This effect increases with a mass difference of the measured particle pair. Hence studying correlations in the $\pi - \Xi$ system where the mass difference is really big should provide rather sensitive test of the emission asymmetries introduced by the transverse expansion of the bulk matter.

Moreover, in addition to the Coulomb interaction studied in the $\pi - K$ system the small relative momentum $\pi^\pm - \Xi^\mp$ correlations may provide sufficiently clear signal of the strong interaction revealing itself via $\Xi^*(1530)$ resonance. Expressing particle momentum in the pair rest frame $\mathbf{k}^* = \mathbf{p}_\pi = -\mathbf{p}_\Xi$ via pair invariant mass $M_{\pi\Xi}$ and m_π and m_Ξ

$$k^* = \frac{[M_{\pi\Xi}^2 - (m_\pi - m_\Xi)^2]^{1/2} [M_{\pi\Xi}^2 - (m_\pi + m_\Xi)^2]^{1/2}}{2M_{\pi\Xi}} \quad (1)$$

one expects the $\Xi^*(1530)$ peak to show up in the correlation function $C(k^*)$ at $k^* \approx 150$ MeV/c. Due to its rather long lifetime $\tau_{\Xi^*(1530)} = 22$ fm/c the resonance could be also a rather sensitive to the $\pi - \Xi$ interaction during long-lived hadronic phase. This should be investigated by both the $\pi - \Xi$ femtoscopy as well as via direct measurements of the $\Xi^*(1530)$ spectra. While first signal of the Ξ^* resonance in heavy ion collision was seen in femtoscopy analysis just two years ago [24] first preliminary STAR measurements concerning the Ξ^* spectra and their yields were presented only recently at the Quark Matter conference in Shanghai this year [25].

A. Data selection

Though in previous analyses [5, 11, 12, 24] the $\pi - \Xi$ correlations were studied for two different system d+Au and Au+Au and also at two different energies in this contribution I will concentrate on Au+Au data at $\sqrt{s_{NN}} = 200$ GeV from RHIC Run IV only. The data were divided into several centrality classes. During the run central trigger was used to enhance fraction of 10% most central events. Track-level cuts based on dE/dx particle identification in the STAR Time Projection Chamber were used. Pion sample momenta p_t were limited to [0.125, 1.] GeV/c. After the dE/dx cuts the upper p_T -limit is 0.8 GeV/c and 0.6 GeV/c at $y = 0$. and $y = 0.8$, respectively. Charged Ξ were reconstructed topologically in the p_t range [0.7, 3.] GeV/c. To increase total number of analyzed $\pi - \Xi$ pairs in this analysis we have used wider rapidity cut then in the previous STAR femtoscopy analyses [26]. The cut $|y| < 0.8$ instead of $|y| < 0.5$ was employed for both particle species. Total number of extracted Ξ used in this analysis are given in Table I.

TABLE I: 200GeV Au+Au, Run IV data set

Centrality	No. of Ξ^\pm	No. of Ξ^-	No. of Ξ^+
0 - 10%	1084×10^3	595×10^3	489×10^3
10 - 40%	412×10^3	226×10^3	186×10^3
40 - 80%	145×10^3	79×10^3	66×10^3

B. Data analysis and corrections

Event mixing technique was used to obtain uncorrelated two-particle distribution in pair rest frame. To remove spurious correlations of non-femtoscopic origin the uncorrelated pairs were constructed from events with sufficient proximity in primary vertex position along the beam direction, multiplicity and event plane orientation variables. Pair cuts were used to remove effects of track splitting and merging. Resulting raw correlation function was then corrected for purity of both particle species. The correction was performed individually for each bin in $\mathbf{k}^* = (k^*, \cos\theta, \phi)$ of the 3-dimensional (3D) correlation function as described below.

C. Pair purity analysis

Pair purity defined as a fraction of primary $\pi - \Xi$ pairs is calculated as a product of particle purities of both particle species. Ξ purity was obtained from reconstructed Ξ invariant mass plot as a function of transverse momentum. Pion purity was estimated using parameter $\sqrt{\lambda}$ of the standard parametrization of the identical $\pi - \pi$ correlation function. The identical pion measurements were performed with the same pion cuts as those used in the $\pi - \Xi$ analysis. Since value of the λ parameter is influenced by decays of long-lived resonance as well as by non-Gaussian shape of the correlation function the pion purity correction can be a significant source of the systematic error.

In order to make contact with previous STAR identical pion analyses [26] on Fig. 1 we present k_T -dependence of parameters λ , R_{out} , R_{side} and R_{long} entering standard outside-long decomposition of 3D correlation function $C(\mathbf{q}) = 1 + \lambda \cdot \exp(-q_{out}^2 R_{out}^2 - q_{side}^2 R_{side}^2 - q_{long}^2 R_{long}^2)$. Here $k_T = (|\mathbf{p}_{1T}| + |\mathbf{p}_{2T}|)/2$ is average transverse momentum of two pions. On the same figure the ratio R_{out}/R_{side} is plotted too. We conclude that the improved cuts used in the present analysis do not change the values of extracted parameters but due to increased acceptance in rapidity and transverse momenta of the pions our analysis covers also region of lower k_T .

We have also studied influence of electrons on purity of the pion sample. Exclusion of pions with dE/dx within $\pm 2\sigma$ around the electron band has changed the value of parameter λ in the k_T interval [0.15, 0.25] GeV/c by 50% at maximum. However the other parameters characterizing the 3D correlation function of identical pions (the radii $R_{out}, R_{side}, R_{long}$) as well as the $\pi - \Xi$ correlation functions remained unchanged.

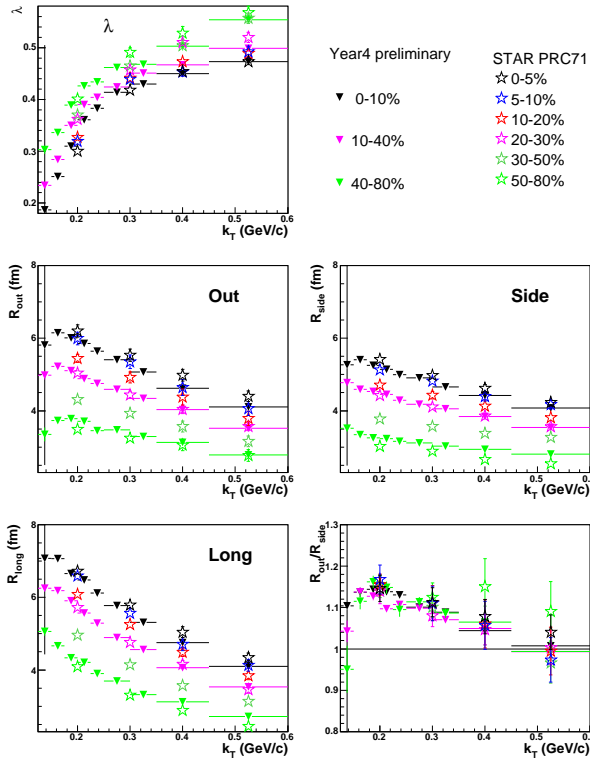


FIG. 1: Comparison between parameters of 3D Gaussian fit the correlation functions of identical charged pions produced in Au+Au collisions at 200 GeV. Previous [26] (open stars) and this analysis (full triangles). Error bars contain only statistical uncertainties.

D. Results in 1D source size information

The $\pi - \Xi$ correlation functions $C(k^*)$ were analyzed in the pair rest frame ($\mathbf{k}^* = \mathbf{p}_\pi = -\mathbf{p}_\Xi$). The results for unlike sign pairs are presented on Fig 2.

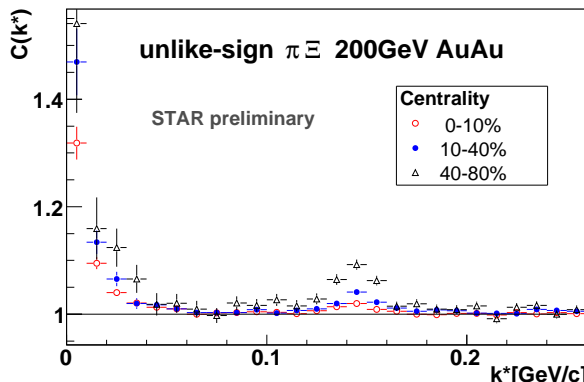


FIG. 2: The centrality dependence of the correlation function of combined sample of unlike-sign $\pi^\pm\Xi^\mp$ pairs.

For all centralities the low k^* region is dominated by the Coulomb interaction. The strong interaction manifest itself in a peak around $k^* \approx 150$ MeV/c corresponding to $\Xi^*(1530)$. Peak's centrality dependence clearly shows high sensitivity to the source size. Contrary to the Coulomb region the correla-

tion function in the resonance region does not suffer from the low statistics and can thus in principle be used to extract sizes of the sources more effectively then in the former case.

E. Results in 3D asymmetry measurement

The information about shift in average emission points between π and Ξ can be extracted from the angular part of the 3D correlation function $C(\mathbf{k}^*) \equiv C(k^*, \cos\theta, \phi)$.

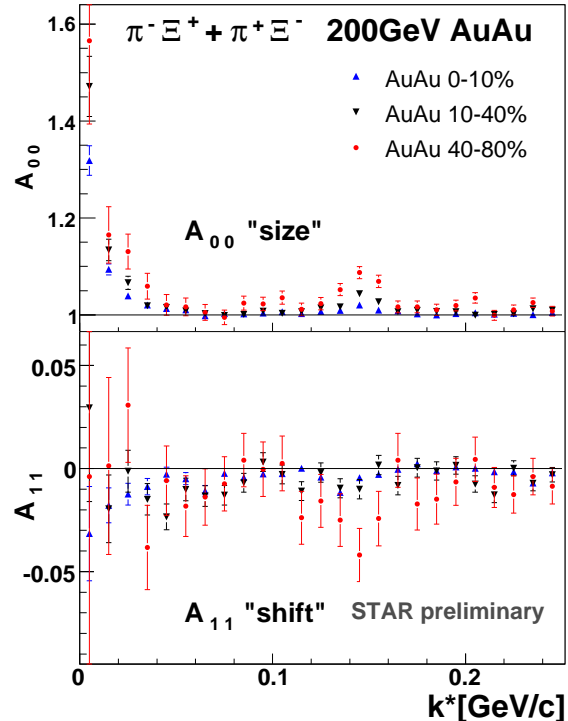


FIG. 3: $A_{00}(k^*)$ and $A_{11}(k^*)$ coefficients of spherical decomposition for combined sample of unlike-sign $\pi^\pm\Xi^\mp$ pairs from three different centrality bins

The function is binned in $k^*, \cos\theta, \phi$ with $\Delta_{\cos\theta} = \frac{2}{N_{\cos\theta}}$ and $\Delta_\phi = \frac{2\pi}{N_\phi}$ as bin sizes in $\cos\theta$ and ϕ , respectively. After its decomposition into spherical harmonics [27]

$$A_{lm}(k^*) = \frac{\Delta_{\cos\theta}\Delta_\phi}{\sqrt{4\pi}} \sum_i^{all \, bins} Y_{lm}(\theta_i, \phi_i) C(k^*, \cos\theta_i, \phi_i) \quad (2)$$

symmetry constrains further limit number of relevant components. This is due to the fact that individual coefficients appearing in the above decomposition represent different symmetries of the source. Thus for azimuthally symmetric identical particle source at midrapidity, only A_{lm} with even values of l and m do not vanish. On the other hand for non-identical particle correlations the coefficients with odd values of l and m are allowed.

For both cases most important coefficient is $A_{00}(k^*)$ representing angle-averaged correlation function $C(k^*)$. Latter is

sensitive to the source size only. On the other hand in non-identical particle case $A_{11}(k^*)$ measures a shift of the average emission point in the R_{out} direction.

The decomposition of the correlation function into spherical harmonics was used to study the centrality dependence of asymmetry in emission between pions and Ξ . The results are presented on Fig 3. The coefficient A_{11} which is non-zero in all centrality bins clearly confirms that the average space-time emission points of pions and Ξ are not the same.

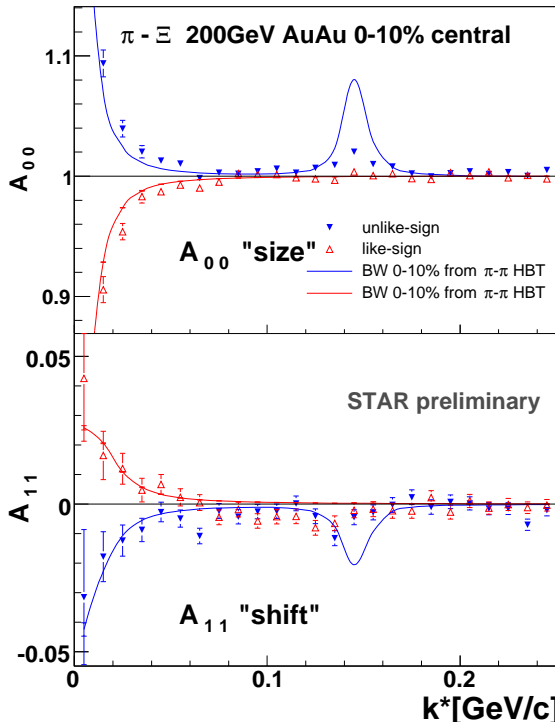


FIG. 4: Comparison of $A_{00}(k^*)$ and $A_{11}(k^*)$ coefficients of spherical decomposition for combined sample of unlike-sign $\pi^{\pm}\Xi^{\mp}$ pairs from 10% most central Au+Au collisions with the FSI model predictions.

On Fig. 4 the experimental results for the 10% most central, the highest statistics bin are compared to a model calculation exploiting strong and Coulomb final state interaction [28]. Theoretical correlation function was constructed from particle emission separation distribution. For this purpose momenta of real particles were used. The emission coordinates of both π and Ξ were generated using the blast wave model [18]. This model encompassing correlation between particle momenta and their space-time coordinates was used with a single set of parameters when generating emission coordinates of both π and Ξ . These parameters were obtained from experimentally measured pion spectra and $\pi - \pi$ emission radii. Let us note that using the same set of parameters for the Ξ source as for the pions implicitly assumes significant transverse flow of Ξ . In the Coulomb region theoretical correlation function is in qualitative agreement with the data. Moreover, orientation of the shift and its magnitude agrees with the scenario in which Ξ participates in transverse expansion. However, in the

region dominated by the strong final state interaction the calculations over predict both, the size and the shift coefficients.

F. Extracting the source parameters

For further analysis we have used only the low k^* region dominated by the Coulomb interaction, excluding thus the region around the $\Xi^*(1530)$ peak (see Fig.5).

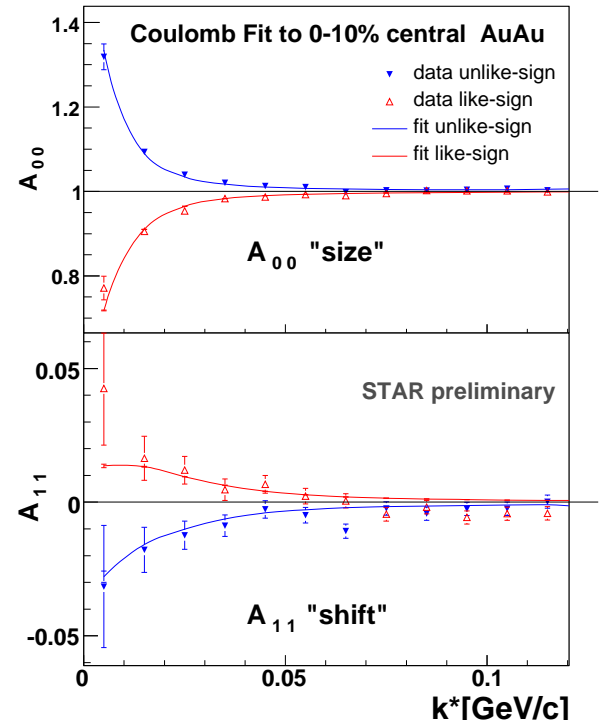


FIG. 5: Comparison of $A_{00}(k^*)$ and $A_{11}(k^*)$ coefficients of spherical decomposition for combined sample of like-sign $\pi^{\pm}\Xi^{\pm}$ and unlike-sign $\pi^{\pm}\Xi^{\mp}$ pairs from 10% most central Au+Au collisions with the FSI model predictions.

The theoretical correlation function was calculated using momentum distribution of pairs extracted from the real data. The emission coordinates were randomly generated from two-parameter source distribution constructed in the following way. For both particle species Gaussian shape of their source was assumed. The sources were shifted in R_{out} direction relative to each other. This in the pair rest frame can be expressed via two parameters R and Δ_{out} characterizing the pair separation distribution Δr^* . R representing the width of the Gaussian and Δ_{out} the shift in the R_{out} direction. Values of the source parameters were then extracted by finding a minimum value of χ^2 between theoretical and real correlation function. Fitting was done simultaneously for like and unlike-sign correlation functions.

For most central Au+Au collision this method yields first preliminary values of $R = (6.7 \pm 1.0)$ fm and $\Delta_{out} = (-5.6 \pm 1.0)$ fm. The errors are purely statistical. Systematic error studies are under way and their values are expected to be of

the order of the statistical ones. In our case a negative value of the shift means that average emission point of Ξ is positioned more to the outside of the whole fire-ball than the average emission point of pion as expected in the Ξ flow scenario.

III. IDENTICAL PION CORRELATIONS

A. Motivation

In ultra-relativistic heavy-ion collisions femtoscopy can also be employed to extract the information related to the strong interaction among the particles [3, 10]. In recent STAR analyses the strong FSI was studied via two- K_s^0 interferometry [29] and in proton-lambda correlations [30]. A model that takes the effect of the strong interaction into account has been used to fit the measured correlation functions. In the $p - \bar{\Lambda}$ and $\bar{p} - \Lambda$ correlations, which were actually measured for the first time, annihilation channels and/or a negative real part of the spin-averaged scattering length was needed in the FSI calculation to reproduce the measured correlation function.

At the previous WPCF meeting ambitious proposal to exploit the correlations among identical charged pions to extract pion-pion scattering lengths was made [8]. Potential for such measurement at RHIC and latter on also at the LHC stems from the fact that compared to a dedicated particle physics experiments measuring scattering lengths parameters a_0^0 and a_0^2 like BNL-E865 [31] or Dirac [32] heavy ion experiments provide much larger number of pion pairs at small relative momenta in a single event plus very large data samples ($10^7 - 10^9$ events). The real challenge when studying the strong interaction among identical charged pions then is to beat down all systematical errors pertinent to ultra-relativistic heavy ion collisions environment. Coulomb interaction, pion purity and geometry of the pion source need to be kept under control. Varying source size (k_T or centrality) may provide a good handle on this.

In particular the bias arising from frequently used Gaussian assumption of the source shape needs to be addressed. Using high statistics sample of Au+Au events from STAR experiment at RHIC highest energy accumulated during the run IV it was found that for all k_T and centrality bins the Lévy stable source parametrization does not bring an advantage in describing the detail shape of measured three-dimensional correlation function [6].

Next step in this direction is to exploit model-independent imaging technique of Brown and Danielewicz [33, 34] and reconstruct the source itself. This is done via inverting Koonin-Pratt equation (see e.g. [1]):

$$C(q) - 1 = 4\pi \int K_0(q, r) S(r) r^2 dr$$

$$K_0(q, r) \equiv \frac{1}{2} \int (|\Phi(\mathbf{q}, \mathbf{r})|^2 - 1) d(\cos \theta_{\mathbf{q}, \mathbf{r}})$$

$$q = \frac{1}{2} \sqrt{-(p_1 - p_2)^2} \quad (3)$$

which expresses the 1D correlation function $C(q)$ in terms of the probability $S(r)$ to emit a pair of particles at a separation

r in the c.m. frame. $S(r)$ is usually called source function. All FSI is encoded in the (angle averaged) final state wave function $\Phi(\mathbf{q}, \mathbf{r})$ describing the propagation of the pair from a relative separation of \mathbf{r} in the pair c.m. to the detector with relative momentum \mathbf{q} . The angle between vectors \mathbf{q} and \mathbf{r} is denoted by $\theta_{\mathbf{q}, \mathbf{r}}$. The procedure to extract $S(r)$ via inversion of Eq. 3 is given in [34].

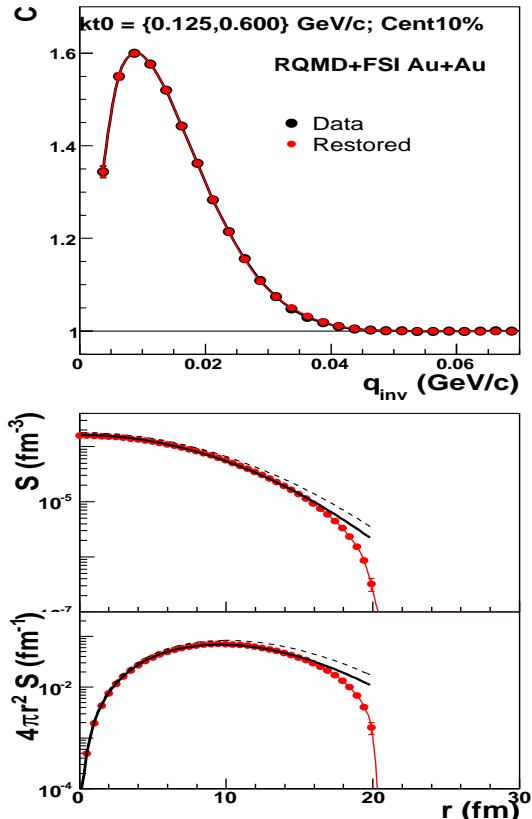


FIG. 6: 1D imaging analysis of isotropic Gaussian source using pion momentum spectra from RQMD simulated 10% most central Au+Au collisions at $\sqrt{s_{NN}} = 200$ GeV. Top: original (black filled circles) and restored by imaging technique (red filled circles) correlation function $C(q)$. To guide an eye the data points are connected by a smooth line of the same color. Middle: 1D source function $S(r)$ (red filled circles). Full black line represents result of a single-Gaussian fit to $S(r)$, dashed line - input Gaussian distribution. Bottom: $4\pi r^2 S(r)$.

B. Testing the inversion procedure

To test reproducibility of original source function by the imaging procedure we have generated Bose-Einstein (B-E) correlated and Coulomb interacting pion pairs. The momentum spectra of the pions were obtained from 10% most central Au+Au RQMD generated events at $\sqrt{s_{NN}} = 200$ GeV. The pions coordinates were randomly sampled from an isotropic 3D Gaussian distribution with the radius $R=5$ fm. The instantaneous emission $\delta\tau=0$ of particles was assumed. Using pion momenta and their coordinates the B-E correlations and

Coulomb FSI were introduced using procedure described in [36]. Results for correlation and the source functions are displayed on Fig.6. In order to compare with the input Gaussian source the extracted source function was fitted with Gaussian distribution again:

$$g(r, R) = \frac{\lambda}{(2\sqrt{\pi}R)^3} e^{-\frac{r^2}{4R^2}} \quad (4)$$

Let us note that the r^2 -weighting of $S(r)$ appearing in the normalization condition of the source function:

$$4\pi \int_0^\infty S(r) r^2 dr = \lambda \quad (5)$$

makes normalization constant λ more sensitive to behavior of $S(r)$ at $r \gg R$ than one would naively expect. Since latter is determined by the imaging from values of the correlation function $C(q)$ at very small q fulfillment of the above normalization condition using data with limited statistics in the low q bins may be hard to achieve. This may explain why the values of extracted parameters R and λ from the single-Gaussian fit were found to be smaller than the input ones. While for R the discrepancy is about 4% for λ it is almost 25%.

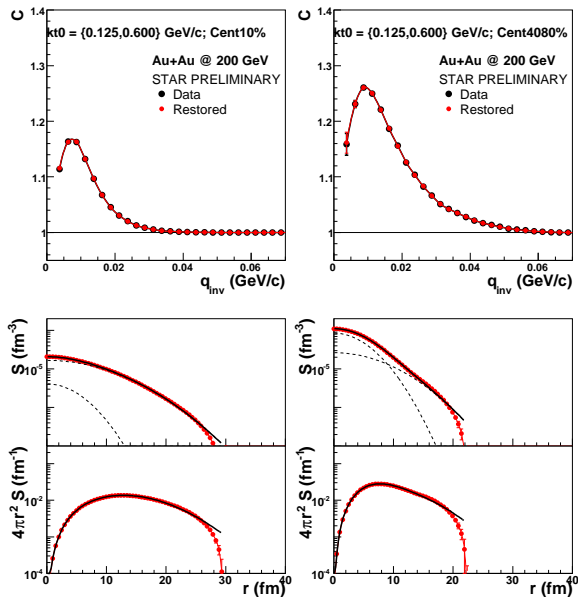


FIG. 7: 1D imaging analysis of identical charged pions from Au+Au collisions at $\sqrt{s_{NN}} = 200$ GeV. Results are shown for 10% most central (the left panel) and for peripheral (centrality 40-80%) collisions (the right panel). Top: measured correlation function $C(q)$ (black filled circles), restored correlation function from imaging technique (red filled circles). To guide an eye the data points are connected by a smooth line of the same color. Middle: 1D source function $S(r)$ (red filled circles). Full black line represents result of a double-Gaussian fit to $S(r)$. Two dashed lines show contribution of each of two Gaussians. Bottom: $4\pi r^2 S(r)$: (red filled circles). Full black line represents result of a double-Gaussian fit.

C. 1D imaging analysis of the pion source from Au+Au and Cu+Cu collisions

The same data set of Au+Au events from Run IV used in already described $\pi - \Xi$ correlation analysis was also used for the reconstruction of the pion source. Second data set employed in imaging analysis consists of about 8 million Cu+Cu minimum bias events at $\sqrt{s_{NN}} = 200$ GeV accumulated during the Run V. Selected results from 1D imaging analysis of the pion source using centrality selected Au+Au and Cu+Cu events are displayed on Fig. 7 and 8, respectively.

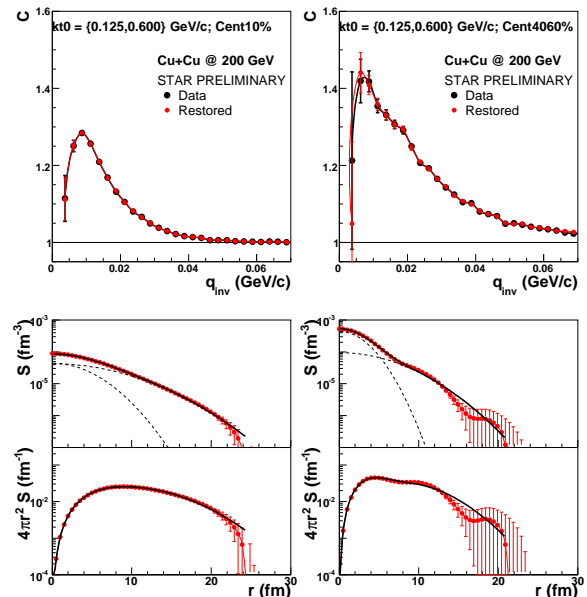


FIG. 8: 1D imaging analysis of identical charged pions from Cu+Cu collisions at $\sqrt{s_{NN}} = 200$ GeV. Results are shown for 10% most central (the left panel) and for peripheral (centrality 40-60%) collisions (the right panel). Top: $C(q)$. Middle: 1D source function $S(r)$. Bottom: $4\pi r^2 S(r)$. Labels are same as on Fig. 7.

Compared to model example discussed in the previous paragraph the extracted source functions now develop long tails [35] and cannot thus be described by a single Gaussian distribution. The only exception are the data from 10% most central Au+Au collisions (Fig.7.) To account for observed behavior we use simplest extension of Eq.4 and assume that the source function obtains contribution from two Gaussians. While the first Gaussian $g(r, R_1)$ contributing with fraction $(1 - \alpha)$ is responsible for the long tails the second one $g(r, R_2)$ contributing with weight α of width the $R_2 < R_1$ describes the source function at small r . The double Gaussian distribution:

$$G(r, R_1, R_2) = (1 - \alpha)g(r, R_1) + \alpha g(r, R_2), R_1 > R_2 \quad (6)$$

now seems to describe data quite well. Comparing Au+Au to Cu+Cu collisions of the same centrality we conclude that the long tails are more pronounced for the smaller system.

All source functions presented so far were obtained from data integrated over the whole range of average pair transverse momenta $k_T = [0.125, 0.600]$ GeV/c). In the following I will present results showing how much observed departure

from a single Gaussian shape depends on particle transverse momenta.

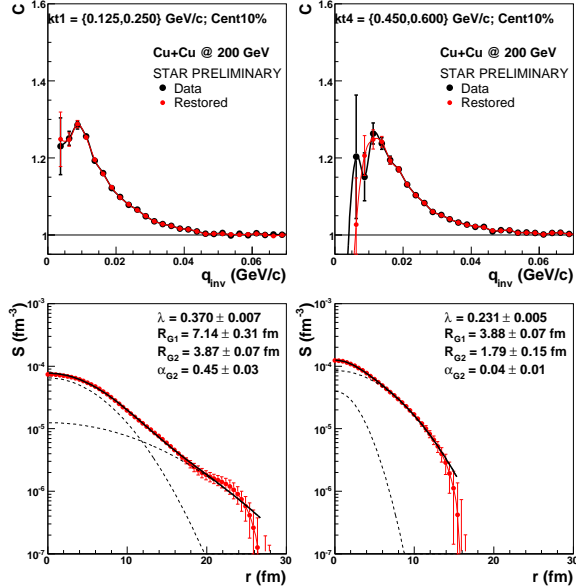


FIG. 9: *1D imaging analysis of identical charged pions from 10% most central Cu+Cu collisions at $\sqrt{s_{NN}} = 200$ GeV. Results shown are for the lowest (the left panel) and for the highest (the right panel) k_T -bin. Top: correlation function $C(q)$. Middle: 1D source function $S(r)$. Bottom: $4\pi r^2 S(r)$. Labels are same as on Fig.7.*

Such analysis is performed on Fig.9-11. While for Au+Au collisions the statistics allowed us to use 9 bins in k_T for Cu+Cu we have used only 4 bins. On Fig.9 the lowest $k_T = [0.125, 0.250]$ GeV/c and the highest $k_T = [0.450, 0.600]$ GeV/c bins from Cu+Cu 10% most central collisions are compared. We see that the long tail present in the lowest k_T bin which is characterized by the Gaussian with the width $R \approx 7$ fm completely disappears from the highest k_T bin.

Fig. 10 and 11 show k_T -dependence of the double Gaussian fit parameters for Cu+Cu and Au+Au collisions at three different centralities, respectively. We observe that with increasing k_T contribution of the second Gaussian is less and less prominent. This behavior is more pronounced in Cu+Cu collisions. Let us note that long tails observed in the low- k_T bins, then may indicate an important rôle played by the pions from long-lived resonance decays. An interesting observation which may have some relevance to observed behavior regarding a random walk nature of the particle freeze-out in coordinate space was made by T. Csörgö at this meeting [37].

IV. SUMMARY

High-statistics STAR data from Au+Au and Cu+Cu collisions taken at full RHIC energy and three different centralities were used to discuss recent progress in identical ($\pi - \pi$) and non-identical ($\pi - \Xi$) particle femtoscopy. In $\pi - \Xi$ system the strong and Coulomb-induced FSI effects are observed making it possible for the first time to estimate the average

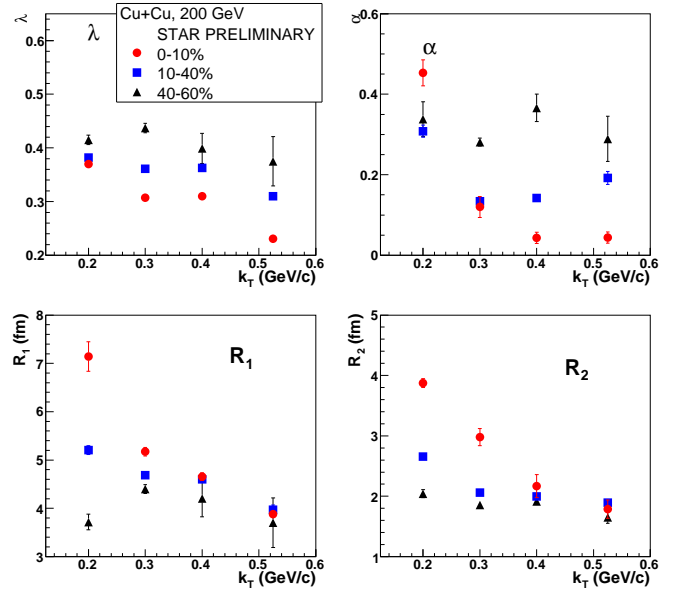


FIG. 10: *k_T -dependence of the source parameters of identical charged pions from Cu+Cu collisions at $\sqrt{s_{NN}} = 200$ GeV taken at three different centralities: 0-10% - full red circles, 10-40% - full blue squares, 40-60% - full black triangles.*

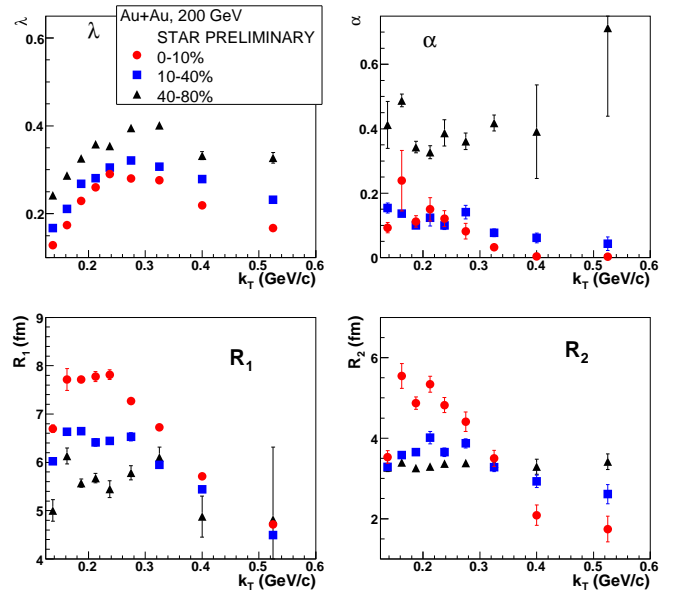


FIG. 11: *k_T -dependence of the source parameters of identical charged pions from Au+Au collisions at $\sqrt{s_{NN}} = 200$ GeV taken at three different centralities: 0-10% - full red circles, 10-40% - full blue squares, 40-80% - full black triangles.*

shift and width between π and Ξ source. 1D imaging of identical pion source reveals significant departure from a single Gaussian shape. Observed long tails which could be fairly well described by allowing for the second Gaussian are more pronounced for the sources produced at large impact parameters. The effect is stronger for Cu+Cu then for Au+Au col-

lisions. For all centralities and both colliding systems the highest departure from single Gaussian shape is observed for sources emitting particle with a small average pair transverse momenta k_T . For highest analyzed k_T the source is to a good approximation a single Gaussian.

Acknowledgements

This work was supported in part by the IRP AV0Z10480505

and by GACR grants 202/04/0793 and 202/07/0079. The data analysis was performed by Michal Bysterský and Petr Chaloupka as a part of their Ph.D. thesis work. I would like to thank to both of them for important input to my talk. My gratitude goes also to the organizers of this excellent meeting, in particular to Sandra Padula.

[1] M. A. Lisa, S. Pratt, R. Soltz and U. Wiedemann, *Ann. Rev. Nucl. Part. Sci.* **55**, 357 (2005) [arXiv:nucl-ex/0505014].

[2] Proc. XXXV Int. Symp. on Multiparticle Dynamics (ISMD 2005), Kroměříž, Czech Republic, August 9-15, 2005 and of the Workshop on Particle Correlations and Femtoscopy (WPCF 2005), Kroměříž, Czech Republic, August 15-17, 2005. Edited by V. Šimák, M. Šumbera, Š. Todorova, B. Tomášik, AIP Conference Proceedings 828, 2006, ISBN 0-7354-0320-1.

[3] R. Lednický, *ibid* p.423.

[4] M. Lisa, *ibid* p.226.

[5] P. Chaloupka, *ibid* p.610.

[6] M. Bysterský, *ibid* p.205; e-Print Archive: nucl-ex/0511053.

[7] R. Lednický, Proc. CIPPCG'01, Palaiseau, France, arXiv: nucl-th/0112011; *Phys. Atom. Nucl.* **67**, 72 (2004).

[8] M. Bysterský and F. Retiere: "Measuring scattering length at STAR," unpublished talk at WPCF 2005. Available at <http://www.particle.cz/conferences/wpcf2005/talks/retiere.ppt>.

[9] Proc. 18th Int. Conf. on Ultra-Relativistic Nucleus-Nucleus Collisions, Budapest, Hungary, 4-9 August, 2005, edited by T. Csörgő, G. Dávid and P. Lévai, *Nucl. Phys. A* **774** (2006).

[10] R. Lednický, *ibid* 189-198.

[11] P. Chaloupka, *ibid* 603-606.

[12] P. Chaloupka, Proc. SQM 2006 Int. Conf. on Strangeness in quark matter, University of California Los Angeles, 2631 March 2006, edited by Kenneth Barish, Huan Zhong Huang, Joseph Kapusta, Grazyna Odyniec, Johann Rafelski and Charles A. Whitten Jr, *J. Phys. G: Nucl. Part. Phys.* **32** S537-S540 (2006).

[13] J. Adams *et al.* [STAR Collaboration], *Nucl. Phys. A* **757** (2005) 102.

[14] B. I. Abelev *et al.* [STAR Collaboration], arXiv:nucl-ex/0607012.

[15] J. Adams *et al.* [STAR Collaboration], *Phys. Rev. Lett.* **95**, 122301 (2005).

[16] D. Molnar and S. A. Voloshin, *Phys. Rev. Lett.* **91**, 092301 (2003), R. J. Fries, B. Muller, C. Nonaka and S. A. Bass, *Phys. Rev. Lett.* **90**, 202303 (2003).

[17] J. Adams *et al.* [STAR Collaboration], arXiv:nucl-ex/0606014.

[18] F. Retiere and M. A. Lisa, *Phys. Rev. C* **70**, 044907 (2004).

[19] R. Lednický, V. L. Lyuboshits, B. Erazmus, and D. Nouais, *Phys. Lett.* **B373** (1996) 3034.

[20] C. Nonaka and S. A. Bass, *Phys. Rev. C* **75**, 014902 (2007).

[21] U. W. Heinz, *J. Phys. G* **31**, S717 (2005).

[22] C. Blume *et al.* [NA49 Collaboration], *Nucl. Phys. A* **715**, 55 (2003).

[23] J. Adams *et al.* [STAR Collaboration], *Phys. Rev. Lett.* **91**, 262302 (2003).

[24] P. Chaloupka [STAR Collaboration], *Nucl. Phys. A* **749**, 283 (2005).

[25] R. Witt, talk at 19th Int. Conf. on Ultra-Relativistic Nucleus-Nucleus Collisions, Shanghai, China, November 14-20, 2006, arXiv:nucl-ex/0701063

[26] J. Adams *et al.* [STAR Collaboration], *Phys. Rev. C* **71**, 044906 (2005).

[27] Z. Chajecki, T. D. Gutierrez, M. A. Lisa and M. Lopez-Noriega [the STAR Collaboration], arXiv:nucl-ex/0505009.

[28] S. Pratt and S. Petroni, *Phys. Rev. C* **68**, 054901 (2003).

[29] B. I. Abelev [STAR Collaboration], *Phys. Rev. C* **74**, 054902 (2006) and S. Bekele, "Neutral Kaon Correlations in 200 GeV/NN Au+Au collisions at RHIC", proceeding WPCF 2006.

[30] J. Adams *et al.* [STAR Collaboration], arXiv:nucl-ex/0511003.

[31] S. Pislak *et al.* [BNL-E865 Collaboration], *Phys. Rev. Lett.* **87**, 221801 (2001).

[32] B. Adeva *et al.* [DIRAC Collaboration], *Phys. Lett. B* **619**, 50 (2005).

[33] D. A. Brown and P. Danielewicz, *Phys. Lett. B* **398**, 252 (1997).

[34] D. A. Brown and P. Danielewicz, *Phys. Rev. C* **57**, 2474 (1998).

[35] S. S. Adler *et al.* [PHENIX Collaboration], arXiv:nucl-ex/0605032.

[36] R. Lednický and V.L. Lyuboshitz, *Yad. Fiz.* **35**, 1316 (1982) [Sov. J. Nucl. Phys. **35**, 770 (1982)]. Fortran program provided by R. Lednický.

[37] M. Csanad, T. Csorgo and M. Nagy, arXiv:hep-ph/0702032.

Selected results on Strong and Coulomb-induced correlations from the STAR experiment

M. Šumbera* for the STAR Collaboration

Nuclear Physics Institute, Academy of Sciences of the Czech Republic, 250 68 Řež, Czech Republic

Using recent high-statistics STAR data from Au+Au and Cu+Cu collisions at full RHIC energy I discuss strong and Coulomb-induced final state interaction effects on identical ($\pi - \pi$) and non-identical ($\pi - \Xi$) particle correlations. Analysis of $\pi - \Xi$ correlations reveals the strong and Coulomb-induced FSI effects allowing for the first time to estimate space extension of π and Ξ sources and average shift between them. Source imaging technique providing clean separation of these effects from effects due to the source function itself is applied to one-dimensional relative momentum correlation function of identical pions. For low momentum pions and/or non-central collisions large departure from a single-Gaussian shape is observed.

Keywords: heavy ions, femtoscopy

I. INTRODUCTION

Progress in understanding space-time structure of multiparticle production via femtoscopy technique is currently driven by high-statistics data sets accumulated in heavy ion experiments at RHIC and SPS accelerators [1, 2, 3, 4, 10]. In particular ambitious program of the STAR collaboration at RHIC exploiting good particle identification has already provided vast variety of femtoscopy measurements in different identical and non-identical particle systems some of which were actually measured for the first time [4]. This contribution is a progress report on two currently pursued STAR femtoscopy analyses. Both of them were introduced already at the previous WPCF meeting last year in Kroměříž [2]. First focuses on non-identical particle correlations in rather exotic meson-baryon system $\pi^\pm - \Xi^\pm$ [5]. Previous investigations have shown that correlations among these two charged hadrons reveal not only the Coulomb but also the strong final state interaction (FSI) effects [11, 12]. Order of magnitude difference in mass plus $\Delta B=1/\Delta S=2$ gap in baryon/ strangeness quantum numbers makes $\pi - \Xi$ system an important tool to study the interplay between matter flow of on partonic and hadronic level. The second analysis exploits particle correlations in a more conventional system of two identical charged pions [6]. Its aim is to understand the geometry of the source. Ultimate and rather ambitious aspiration of this project is to extract pion-pion scattering lengths. This goal, not reached so far, will make heavy ion femtoscopy measurements fully competitive to a dedicated particle physics experiments trying to extract this important parameter of the strong interactions [3, 7, 8]. Basic prerequisites for such measurements are good knowledge of correlations due to quantum statistics and Coulomb interactions.

II. STUDYING SPACE-TIME STRUCTURE OF MULTI-STRANGE BARYON SOURCE VIA $\pi - \Xi$ CORRELATIONS

In ultra-relativistic heavy-ion collisions at RHIC hot and dense strongly interacting matter is created exhibiting prop-

erties of de-confined partonic matter [9, 13]. Almost instantaneous equilibration of produced matter indicated by recent heavy flavor measurements [9, 14] represent one of the greatest puzzles coming from the RHIC [9]. The early partonic collectivity also shows up in a subsequent evolution of the system leading to strong collective expansion of the bulk matter as demonstrated by large values of observed elliptic flow [9, 13]. These observations are further substantiated by STAR multi-strange baryon measurements showing that Ξ and Ω baryons reveal significant amount of elliptic flow which is comparable to ordinary non-strange baryons [15]. The sizable multi-strange baryon elliptic flow which obeys constituent quark scaling [16] confirms that substantial part of the collective motion has indeed developed prior to hadronization. This picture is also corroborated by more recent STAR analysis of the centrality dependence of hyperon yields carried out within the framework of a thermal model [17]. Observed scaling behavior of strange baryons is consistent with a scenario of hadron formation from constituent quark degrees of freedom through quark recombination provided that the coalescence took place over a volume that is much larger than the one created in any elementary collisions.

These observations fit nicely into ideal hydro evolution starting from the system of de-confined QCD matter. However they are also consistent with more realistic hybrid macroscopic/microscopic transport approach [20] which takes into account the strength of dissipative effects prevalent in the latter hadronic phase of the reaction. The hybrid model calculations indicate that at top RHIC energy the hadronic phase of the heavy-ion reaction is of significant duration (at least 10 fm/c) making hadronic freeze-out a continuous process, strongly depending on hadron flavor and momenta. In particular heavy hadrons, which are quite sensitive to radial flow effects, obtain the additional collective push created by resonant (quasi)elastic interactions during that fairly long-lived hadronic rescattering stage [21].

It is clear that question concerning multi-strange baryon decoupling from hot and strongly interacting partonic/hadronic system is an interesting one but also not an easy one to solve. Could this be provided by the femtoscopy? What kind of relevant information can be obtained via low-relative-velocity correlations of multi-strange baryons with the other hadrons? Since non-identical particle correlations are sensitive not only to the extent of the source, but also

*e-mail: sumbera@ujf.cas.cz

to the average shift in emission time and position among different particle species [19] the answer is affirmative. The femtoscopy of non-identical particles was already used to show that the average emission points of pions, kaons and protons produced in heavy-ion collisions at SPS and RHIC are not the same [3, 7, 10, 22, 23]. In hydrodynamically inspired blast-wave approach [18] mass ordering of average space-time emission points of different particle species naturally appears due to the transverse expansion of the source. This effect increases with a mass difference of the measured particle pair. Hence studying correlations in the $\pi - \Xi$ system where the mass difference is really big should provide rather sensitive test of the emission asymmetries introduced by the transverse expansion of the bulk matter.

Moreover, in addition to the Coulomb interaction studied in the $\pi - K$ system the small relative momentum $\pi^\pm - \Xi^\mp$ correlations may provide sufficiently clear signal of the strong interaction revealing itself via $\Xi^*(1530)$ resonance. Expressing particle momentum in the pair rest frame $\mathbf{k}^* = \mathbf{p}_\pi = -\mathbf{p}_\Xi$ via pair invariant mass $M_{\pi\Xi}$ and m_π and m_Ξ

$$k^* = \frac{[M_{\pi\Xi}^2 - (m_\pi - m_\Xi)^2]^{1/2} [M_{\pi\Xi}^2 - (m_\pi + m_\Xi)^2]^{1/2}}{2M_{\pi\Xi}} \quad (1)$$

one expects the $\Xi^*(1530)$ peak to show up in the correlation function $C(k^*)$ at $k^* \approx 150$ MeV/c. Due to its rather long lifetime $\tau_{\Xi^*(1530)} = 22$ fm/c the resonance could be also a rather sensitive to the $\pi - \Xi$ interaction during long-lived hadronic phase. This should be investigated by both the $\pi - \Xi$ femtoscopy as well as via direct measurements of the $\Xi^*(1530)$ spectra. While first signal of the Ξ^* resonance in heavy ion collision was seen in femtoscopy analysis just two years ago [24] first preliminary STAR measurements concerning the Ξ^* spectra and their yields were presented only recently at the Quark Matter conference in Shanghai this year [25].

A. Data selection

Though in previous analyses [5, 11, 12, 24] the $\pi - \Xi$ correlations were studied for two different system d+Au and Au+Au and also at two different energies in this contribution I will concentrate on Au+Au data at $\sqrt{s_{NN}} = 200$ GeV from RHIC Run IV only. The data were divided into several centrality classes. During the run central trigger was used to enhance fraction of 10% most central events. Track-level cuts based on dE/dx particle identification in the STAR Time Projection Chamber were used. Pion sample momenta p_t were limited to [0.125, 1.] GeV/c. After the dE/dx cuts the upper p_T -limit is 0.8 GeV/c and 0.6 GeV/c at $y = 0$. and $y = 0.8$, respectively. Charged Ξ were reconstructed topologically in the p_t range [0.7, 3.] GeV/c. To increase total number of analyzed $\pi - \Xi$ pairs in this analysis we have used wider rapidity cut then in the previous STAR femtoscopy analyses [26]. The cut $|y| < 0.8$ instead of $|y| < 0.5$ was employed for both particle species. Total number of extracted Ξ used in this analysis are given in Table I.

TABLE I: 200GeV Au+Au, Run IV data set

Centrality	No. of Ξ^\pm	No. of Ξ^-	No. of Ξ^+
0 - 10%	1084×10^3	595×10^3	489×10^3
10 - 40%	412×10^3	226×10^3	186×10^3
40 - 80%	145×10^3	79×10^3	66×10^3

B. Data analysis and corrections

Event mixing technique was used to obtain uncorrelated two-particle distribution in pair rest frame. To remove spurious correlations of non-femtoscopic origin the uncorrelated pairs were constructed from events with sufficient proximity in primary vertex position along the beam direction, multiplicity and event plane orientation variables. Pair cuts were used to remove effects of track splitting and merging. Resulting raw correlation function was then corrected for purity of both particle species. The correction was performed individually for each bin in $\mathbf{k}^* = (k^*, \cos\theta, \phi)$ of the 3-dimensional (3D) correlation function as described below.

C. Pair purity analysis

Pair purity defined as a fraction of primary $\pi - \Xi$ pairs is calculated as a product of particle purities of both particle species. Ξ purity was obtained from reconstructed Ξ invariant mass plot as a function of transverse momentum. Pion purity was estimated using parameter $\sqrt{\lambda}$ of the standard parametrization of the identical $\pi - \pi$ correlation function. The identical pion measurements were performed with the same pion cuts as those used in the $\pi - \Xi$ analysis. Since value of the λ parameter is influenced by decays of long-lived resonance as well as by non-Gaussian shape of the correlation function the pion purity correction can be a significant source of the systematic error.

In order to make contact with previous STAR identical pion analyses [26] on Fig. 1 we present k_T -dependence of parameters λ , R_{out} , R_{side} and R_{long} entering standard outside-long decomposition of 3D correlation function $C(\mathbf{q}) = 1 + \lambda \cdot \exp(-q_{out}^2 R_{out}^2 - q_{side}^2 R_{side}^2 - q_{long}^2 R_{long}^2)$. Here $k_T = (|\mathbf{p}_{1T}| + |\mathbf{p}_{2T}|)/2$ is average transverse momentum of two pions. On the same figure the ratio R_{out}/R_{side} is plotted too. We conclude that the improved cuts used in the present analysis do not change the values of extracted parameters but due to increased acceptance in rapidity and transverse momenta of the pions our analysis covers also region of lower k_T .

We have also studied influence of electrons on purity of the pion sample. Exclusion of pions with dE/dx within $\pm 2\sigma$ around the electron band has changed the value of parameter λ in the k_T interval [0.15, 0.25] GeV/c by 50% at maximum. However the other parameters characterizing the 3D correlation function of identical pions (the radii $R_{out}, R_{side}, R_{long}$) as well as the $\pi - \Xi$ correlation functions remained unchanged.

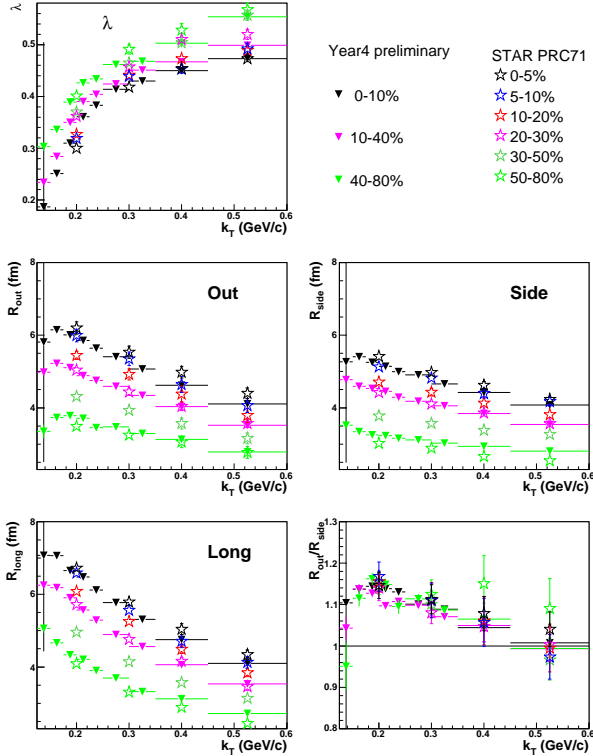


FIG. 1: Comparison between parameters of 3D Gaussian fit the correlation functions of identical charged pions produced in Au+Au collisions at 200 GeV. Previous [26] (open stars) and this analysis (full triangles). Error bars contain only statistical uncertainties.

D. Results in 1D source size information

The $\pi - \Xi$ correlation functions $C(k^*)$ were analyzed in the pair rest frame ($\mathbf{k}^* = \mathbf{p}_\pi = -\mathbf{p}_\Xi$). The results for unlike sign pairs are presented on Fig 2.

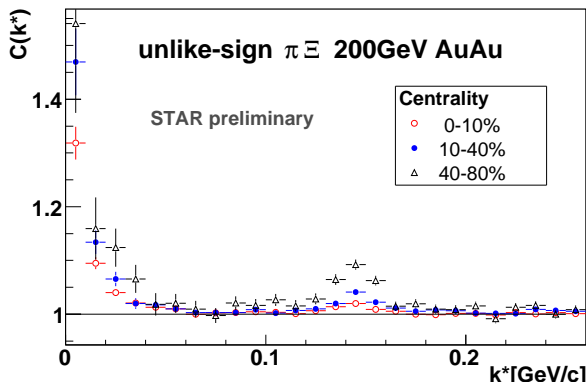


FIG. 2: The centrality dependence of the correlation function of combined sample of unlike-sign $\pi^\pm\Xi^\mp$ pairs.

For all centralities the low k^* region is dominated by the Coulomb interaction. The strong interaction manifest itself in a peak around $k^* \approx 150$ MeV/c corresponding to $\Xi^*(1530)$. Peak's centrality dependence clearly shows high sensitivity to the source size. Contrary to the Coulomb region the correla-

tion function in the resonance region does not suffer from the low statistics and can thus in principle be used to extract sizes of the sources more effectively then in the former case.

E. Results in 3D asymmetry measurement

The information about shift in average emission points between π and Ξ can be extracted from the angular part of the 3D correlation function $C(\mathbf{k}^*) \equiv C(k^*, \cos\theta, \phi)$.

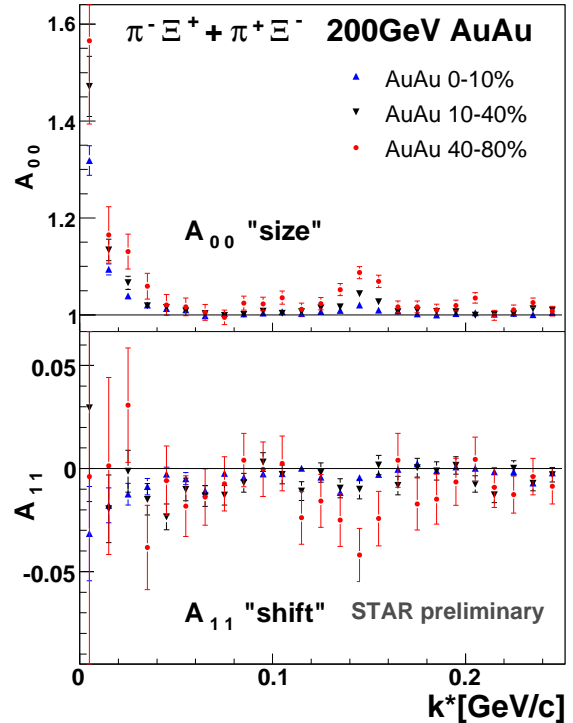


FIG. 3: $A_{00}(k^*)$ and $A_{11}(k^*)$ coefficients of spherical decomposition for combined sample of unlike-sign $\pi^\pm\Xi^\mp$ pairs from three different centrality bins

The function is binned in $k^*, \cos\theta, \phi$ with $\Delta_{\cos\theta} = \frac{2}{N_{\cos\theta}}$ and $\Delta_\phi = \frac{2\pi}{N_\phi}$ as bin sizes in $\cos\theta$ and ϕ , respectively. After its decomposition into spherical harmonics [27]

$$A_{lm}(k^*) = \frac{\Delta_{\cos\theta}\Delta_\phi}{\sqrt{4\pi}} \sum_i^{all\ bins} Y_{lm}(\theta_i, \phi_i) C(k^*, \cos\theta_i, \phi_i) \quad (2)$$

symmetry constrains further limit number of relevant components. This is due to the fact that individual coefficients appearing in the above decomposition represent different symmetries of the source. Thus for azimuthally symmetric identical particle source at midrapidity, only A_{lm} with even values of l and m do not vanish. On the other hand for non-identical particle correlations the coefficients with odd values of l and m are allowed.

For both cases most important coefficient is $A_{00}(k^*)$ representing angle-averaged correlation function $C(k^*)$. Latter is

sensitive to the source size only. On the other hand in non-identical particle case $A_{11}(k^*)$ measures a shift of the average emission point in the R_{out} direction.

The decomposition of the correlation function into spherical harmonics was used to study the centrality dependence of asymmetry in emission between pions and Ξ . The results are presented on Fig 3. The coefficient A_{11} which is non-zero in all centrality bins clearly confirms that the average space-time emission points of pions and Ξ are not the same.

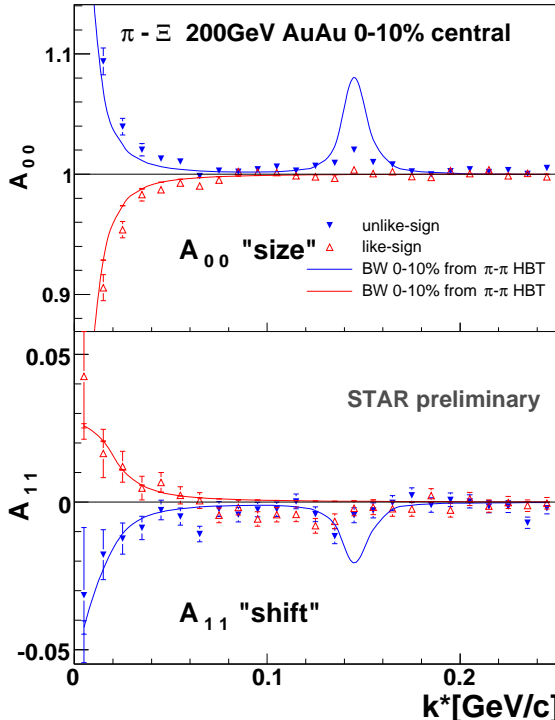


FIG. 4: Comparison of $A_{00}(k^*)$ and $A_{11}(k^*)$ coefficients of spherical decomposition for combined sample of unlike-sign $\pi^{\pm}\Xi^{\mp}$ pairs from 10% most central Au+Au collisions with the FSI model predictions.

On Fig. 4 the experimental results for the 10% most central, the highest statistics bin are compared to a model calculation exploiting strong and Coulomb final state interaction [28]. Theoretical correlation function was constructed from particle emission separation distribution. For this purpose momenta of real particles were used. The emission coordinates of both π and Ξ were generated using the blast wave model [18]. This model encompassing correlation between particle momenta and their space-time coordinates was used with a single set of parameters when generating emission coordinates of both π and Ξ . These parameters were obtained from experimentally measured pion spectra and $\pi - \pi$ emission radii. Let us note that using the same set of parameters for the Ξ source as for the pions implicitly assumes significant transverse flow of Ξ . In the Coulomb region theoretical correlation function is in qualitative agreement with the data. Moreover, orientation of the shift and its magnitude agrees with the scenario in which Ξ participates in transverse expansion. However, in the

region dominated by the strong final state interaction the calculations over predict both, the size and the shift coefficients.

F. Extracting the source parameters

For further analysis we have used only the low k^* region dominated by the Coulomb interaction, excluding thus the region around the $\Xi^*(1530)$ peak (see Fig.5).

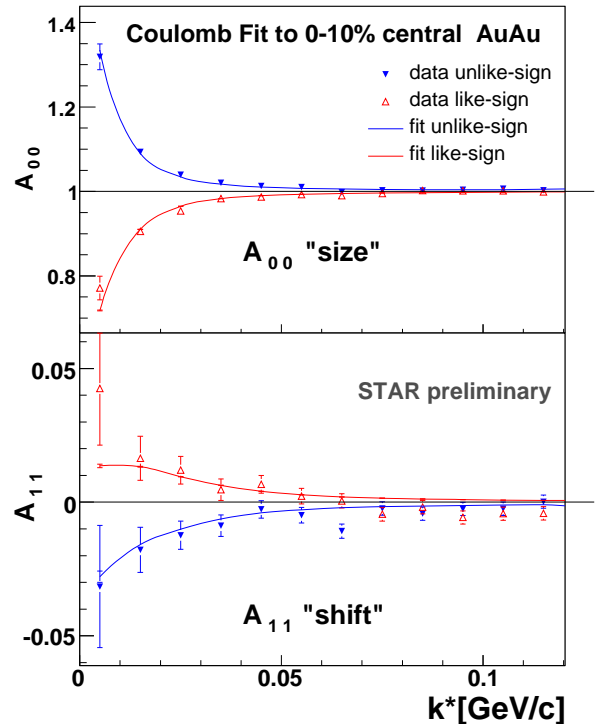


FIG. 5: Comparison of $A_{00}(k^*)$ and $A_{11}(k^*)$ coefficients of spherical decomposition for combined sample of like-sign $\pi^{\pm}\Xi^{\pm}$ and unlike-sign $\pi^{\pm}\Xi^{\mp}$ pairs from 10% most central Au+Au collisions with the FSI model predictions.

The theoretical correlation function was calculated using momentum distribution of pairs extracted from the real data. The emission coordinates were randomly generated from two-parameter source distribution constructed in the following way. For both particle species Gaussian shape of their source was assumed. The sources were shifted in R_{out} direction relative to each other. This in the pair rest frame can be expressed via two parameters R and Δ_{out} characterizing the pair separation distribution Δr^* . R representing the width of the Gaussian and Δ_{out} the shift in the R_{out} direction. Values of the source parameters were then extracted by finding a minimum value of χ^2 between theoretical and real correlation function. Fitting was done simultaneously for like and unlike-sign correlation functions.

For most central Au+Au collision this method yields first preliminary values of $R = (6.7 \pm 1.0)$ fm and $\Delta_{out} = (-5.6 \pm 1.0)$ fm. The errors are purely statistical. Systematic error studies are under way and their values are expected to be of

the order of the statistical ones. In our case a negative value of the shift means that average emission point of Ξ is positioned more to the outside of the whole fire-ball than the average emission point of pion as expected in the Ξ flow scenario.

III. IDENTICAL PION CORRELATIONS

A. Motivation

In ultra-relativistic heavy-ion collisions femtoscopy can also be employed to extract the information related to the strong interaction among the particles [3, 10]. In recent STAR analyses the strong FSI was studied via two- K_s^0 interferometry [29] and in proton-lambda correlations [30]. A model that takes the effect of the strong interaction into account has been used to fit the measured correlation functions. In the $p - \bar{\Lambda}$ and $\bar{p} - \Lambda$ correlations, which were actually measured for the first time, annihilation channels and/or a negative real part of the spin-averaged scattering length was needed in the FSI calculation to reproduce the measured correlation function.

At the previous WPCF meeting ambitious proposal to exploit the correlations among identical charged pions to extract pion-pion scattering lengths was made [8]. Potential for such measurement at RHIC and latter on also at the LHC stems from the fact that compared to a dedicated particle physics experiments measuring scattering lengths parameters a_0^0 and a_0^2 like BNL-E865 [31] or Dirac [32] heavy ion experiments provide much larger number of pion pairs at small relative momenta in a single event plus very large data samples ($10^7 - 10^9$ events). The real challenge when studying the strong interaction among identical charged pions then is to beat down all systematical errors pertinent to ultra-relativistic heavy ion collisions environment. Coulomb interaction, pion purity and geometry of the pion source need to be kept under control. Varying source size (k_T or centrality) may provide a good handle on this.

In particular the bias arising from frequently used Gaussian assumption of the source shape needs to be addressed. Using high statistics sample of Au+Au events from STAR experiment at RHIC highest energy accumulated during the run IV it was found that for all k_T and centrality bins the Lévy stable source parametrization does not bring an advantage in describing the detail shape of measured three-dimensional correlation function [6].

Next step in this direction is to exploit model-independent imaging technique of Brown and Danielewicz [33, 34] and reconstruct the source itself. This is done via inverting Koonin-Pratt equation (see e.g. [1]):

$$C(q) - 1 = 4\pi \int K_0(q, r) S(r) r^2 dr$$

$$K_0(q, r) \equiv \frac{1}{2} \int (|\Phi(\mathbf{q}, \mathbf{r})|^2 - 1) d(\cos \theta_{\mathbf{q}, \mathbf{r}})$$

$$q = \frac{1}{2} \sqrt{-(p_1 - p_2)^2} \quad (3)$$

which expresses the 1D correlation function $C(q)$ in terms of the probability $S(r)$ to emit a pair of particles at a separation

r in the c.m. frame. $S(r)$ is usually called source function. All FSI is encoded in the (angle averaged) final state wave function $\Phi(\mathbf{q}, \mathbf{r})$ describing the propagation of the pair from a relative separation of \mathbf{r} in the pair c.m. to the detector with relative momentum \mathbf{q} . The angle between vectors \mathbf{q} and \mathbf{r} is denoted by $\theta_{\mathbf{q}, \mathbf{r}}$. The procedure to extract $S(r)$ via inversion of Eq. 3 is given in [34].

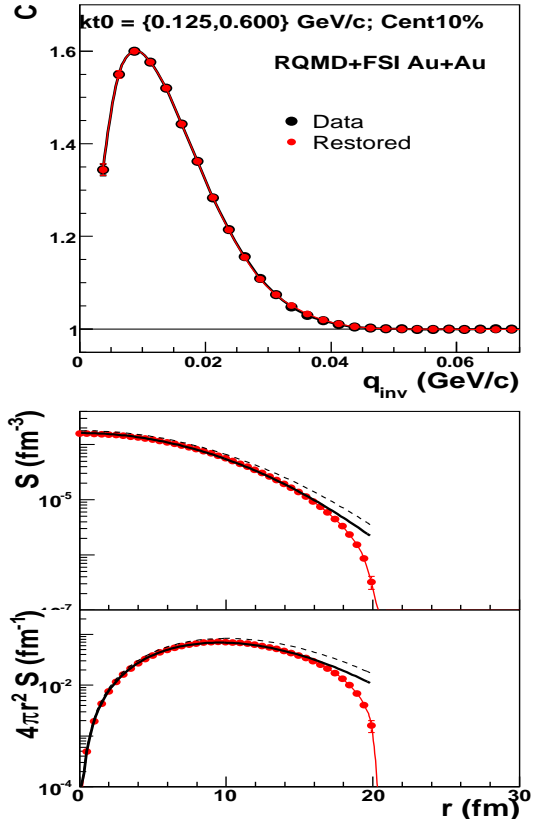


FIG. 6: 1D imaging analysis of isotropic Gaussian source using pion momentum spectra from RQMD simulated 10% most central Au+Au collisions at $\sqrt{s_{NN}} = 200$ GeV. Top: original (black filled circles) and restored by imaging technique (red filled circles) correlation function $C(q)$. To guide an eye the data points are connected by a smooth line of the same color. Middle: 1D source function $S(r)$ (red filled circles). Full black line represents result of a single-Gaussian fit to $S(r)$, dashed line - input Gaussian distribution. Bottom: $4\pi r^2 S(r)$.

B. Testing the inversion procedure

To test reproducibility of original source function by the imaging procedure we have generated Bose-Einstein (B-E) correlated and Coulomb interacting pion pairs. The momentum spectra of the pions were obtained from 10% most central Au+Au RQMD generated events at $\sqrt{s_{NN}} = 200$ GeV. The pions coordinates were randomly sampled from an isotropic 3D Gaussian distribution with the radius $R=5$ fm. The instantaneous emission $\delta\tau=0$ of particles was assumed. Using pion momenta and their coordinates the B-E correlations and

Coulomb FSI were introduced using procedure described in [36]. Results for correlation and the source functions are displayed on Fig.6. In order to compare with the input Gaussian source the extracted source function was fitted with Gaussian distribution again:

$$g(r, R) = \frac{\lambda}{(2\sqrt{\pi}R)^3} e^{-\frac{r^2}{4R^2}} \quad (4)$$

Let us note that the r^2 -weighting of $S(r)$ appearing in the normalization condition of the source function:

$$4\pi \int_0^\infty S(r) r^2 dr = \lambda \quad (5)$$

makes normalization constant λ more sensitive to behavior of $S(r)$ at $r \gg R$ than one would naively expect. Since latter is determined by the imaging from values of the correlation function $C(q)$ at very small q fulfillment of the above normalization condition using data with limited statistics in the low q bins may be hard to achieve. This may explain why the values of extracted parameters R and λ from the single-Gaussian fit were found to be smaller than the input ones. While for R the discrepancy is about 4% for λ it is almost 25%.

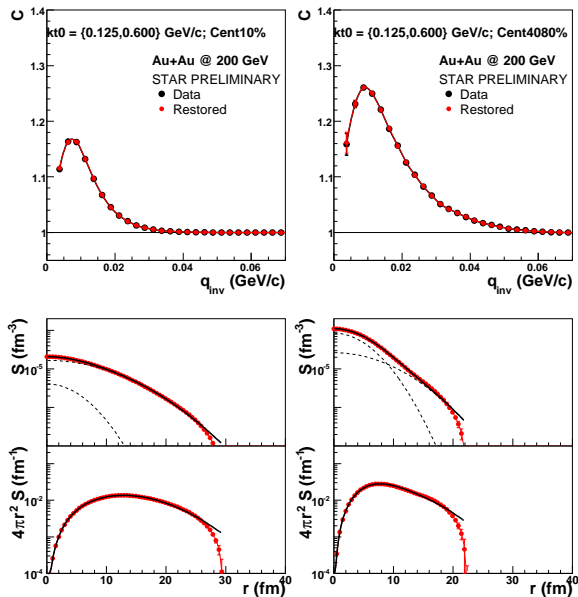


FIG. 7: 1D imaging analysis of identical charged pions from Au+Au collisions at $\sqrt{s_{NN}} = 200$ GeV. Results are shown for 10% most central (the left panel) and for peripheral (centrality 40-80%) collisions (the right panel). Top: measured correlation function $C(q)$ (black filled circles), restored correlation function from imaging technique (red filled circles). To guide an eye the data points are connected by a smooth line of the same color. Middle: 1D source function $S(r)$ (red filled circles). Full black line represents result of a double-Gaussian fit to $S(r)$. Two dashed lines show contribution of each of two Gaussians. Bottom: $4\pi r^2 S(r)$: (red filled circles). Full black line represents result of a double-Gaussian fit.

C. 1D imaging analysis of the pion source from Au+Au and Cu+Cu collisions

The same data set of Au+Au events from Run IV used in already described $\pi - \Xi$ correlation analysis was also used for the reconstruction of the pion source. Second data set employed in imaging analysis consists of about 8 million Cu+Cu minimum bias events at $\sqrt{s_{NN}} = 200$ GeV accumulated during the Run V. Selected results from 1D imaging analysis of the pion source using centrality selected Au+Au and Cu+Cu events are displayed on Fig. 7 and 8, respectively.

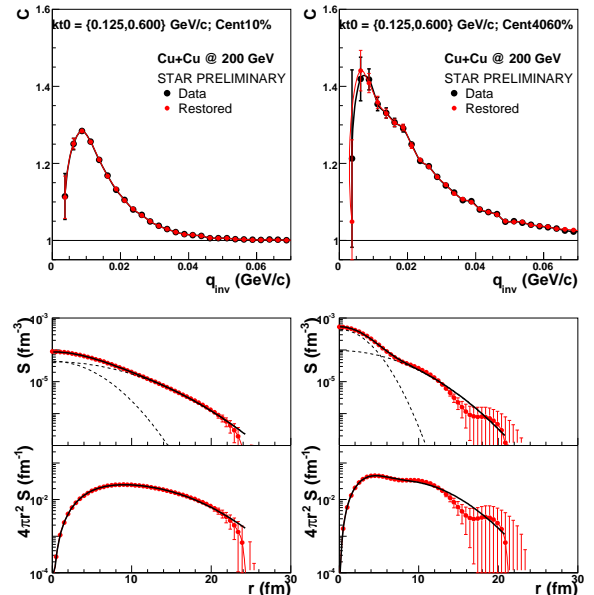


FIG. 8: 1D imaging analysis of identical charged pions from Cu+Cu collisions at $\sqrt{s_{NN}} = 200$ GeV. Results are shown for 10% most central (the left panel) and for peripheral (centrality 40-60%) collisions (the right panel). Top: $C(q)$. Middle: 1D source function $S(r)$. Bottom: $4\pi r^2 S(r)$. Labels are same as on Fig. 7.

Compared to model example discussed in the previous paragraph the extracted source functions now develop long tails [35] and cannot thus be described by a single Gaussian distribution. The only exception are the data from 10% most central Au+Au collisions (Fig.7.) To account for observed behavior we use simplest extension of Eq.4 and assume that the source function obtains contribution from two Gaussians. While the first Gaussian $g(r, R_1)$ contributing with fraction $(1 - \alpha)$ is responsible for the long tails the second one $g(r, R_2)$ contributing with weight α of width the $R_2 < R_1$ describes the source function at small r . The double Gaussian distribution:

$$G(r, R_1, R_2) = (1 - \alpha)g(r, R_1) + \alpha g(r, R_2), R_1 > R_2 \quad (6)$$

now seems to describe data quite well. Comparing Au+Au to Cu+Cu collisions of the same centrality we conclude that the long tails are more pronounced for the smaller system.

All source functions presented so far were obtained from data integrated over the whole range of average pair transverse momenta $k_T = [0.125, 0.600]$ GeV/c). In the following I will present results showing how much observed departure

from a single Gaussian shape depends on particle transverse momenta.

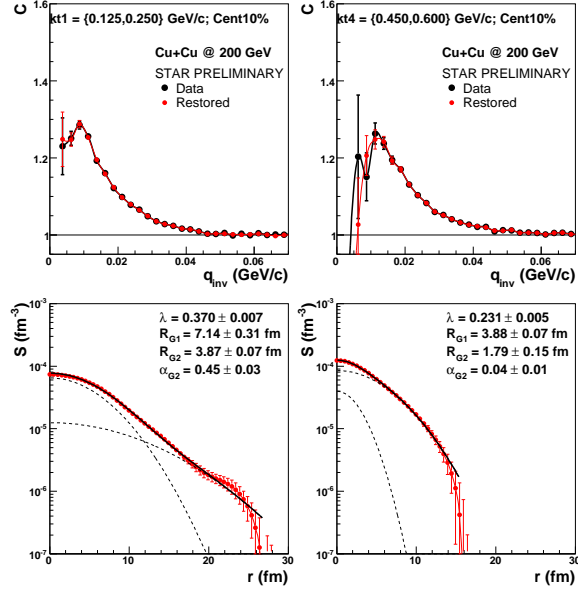


FIG. 9: *1D imaging analysis of identical charged pions from 10% most central Cu+Cu collisions at $\sqrt{s_{NN}} = 200$ GeV. Results shown are for the lowest (the left panel) and for the highest (the right panel) k_T -bin. Top: correlation function $C(q)$. Middle: 1D source function $S(r)$. Bottom: $4\pi r^2 S(r)$. Labels are same as on Fig.7.*

Such analysis is performed on Fig.9-11. While for Au+Au collisions the statistics allowed us to use 9 bins in k_T for Cu+Cu we have used only 4 bins. On Fig.9 the lowest $k_T = [0.125, 0.250]$ GeV/c and the highest $k_T = [0.450, 0.600]$ GeV/c bins from Cu+Cu 10% most central collisions are compared. We see that the long tail present in the lowest k_T bin which is characterized by the Gaussian with the width $R \approx 7$ fm completely disappears from the highest k_T bin.

Fig. 10 and 11 show k_T -dependence of the double Gaussian fit parameters for Cu+Cu and Au+Au collisions at three different centralities, respectively. We observe that with increasing k_T contribution of the second Gaussian is less and less prominent. This behavior is more pronounced in Cu+Cu collisions. Let us note that long tails observed in the low- k_T bins, then may indicate an important rôle played by the pions from long-lived resonance decays. An interesting observation which may have some relevance to observed behavior regarding a random walk nature of the particle freeze-out in coordinate space was made by T. Csörgö at this meeting [37].

IV. SUMMARY

High-statistics STAR data from Au+Au and Cu+Cu collisions taken at full RHIC energy and three different centralities were used to discuss recent progress in identical ($\pi - \pi$) and non-identical ($\pi - \Xi$) particle femtoscopy. In $\pi - \Xi$ system the strong and Coulomb-induced FSI effects are observed making it possible for the first time to estimate the average

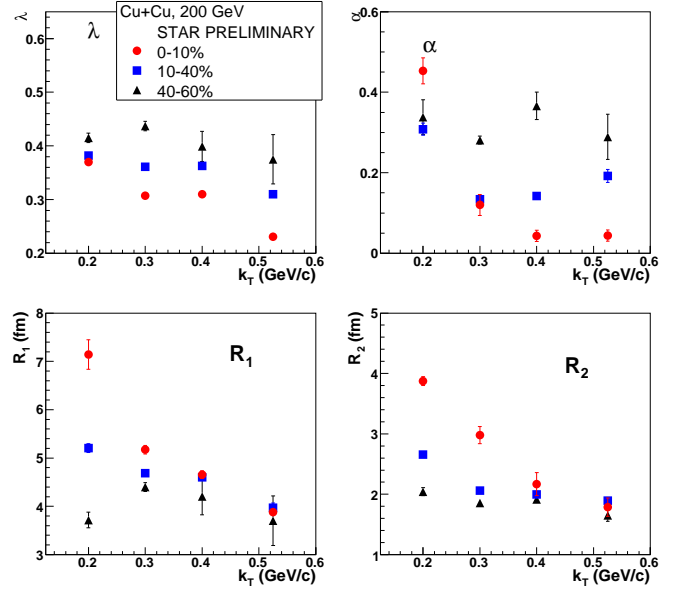


FIG. 10: *k_T -dependence of the source parameters of identical charged pions from Cu+Cu collisions at $\sqrt{s_{NN}} = 200$ GeV taken at three different centralities: 0-10% - full red circles, 10-40% - full blue squares, 40-60% - full black triangles.*

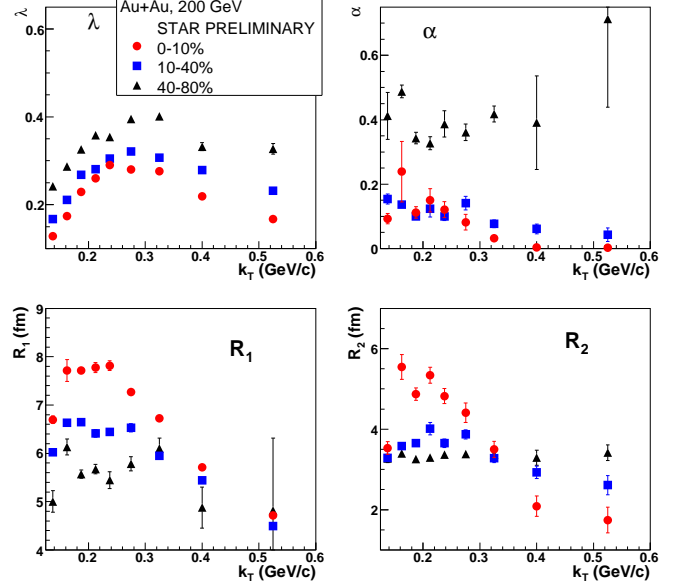


FIG. 11: *k_T -dependence of the source parameters of identical charged pions from Au+Au collisions at $\sqrt{s_{NN}} = 200$ GeV taken at three different centralities: 0-10% - full red circles, 10-40% - full blue squares, 40-80% - full black triangles.*

shift and width between π and Ξ source. 1D imaging of identical pion source reveals significant departure from a single Gaussian shape. Observed long tails which could be fairly well described by allowing for the second Gaussian are more pronounced for the sources produced at large impact parameters. The effect is stronger for Cu+Cu then for Au+Au col-

lisions. For all centralities and both colliding systems the highest departure from single Gaussian shape is observed for sources emitting particle with a small average pair transverse momenta k_T . For highest analyzed k_T the source is to a good approximation a single Gaussian.

Acknowledgements

This work was supported in part by the IRP AV0Z10480505

and by GACR grants 202/04/0793 and 202/07/0079. The data analysis was performed by Michal Bysterský and Petr Chaloupka as a part of their Ph.D. thesis work. I would like to thank to both of them for important input to my talk. My gratitude goes also to the organizers of this excellent meeting, in particular to Sandra Padula.

[1] M. A. Lisa, S. Pratt, R. Soltz and U. Wiedemann, Ann. Rev. Nucl. Part. Sci. **55**, 357 (2005) [arXiv:nucl-ex/0505014].

[2] Proc. XXXV Int. Symp. on Multiparticle Dynamics (ISMD 2005), Kroměříž, Czech Republic, August 9-15, 2005 and of the Workshop on Particle Correlations and Femtoscopy (WPCF 2005), Kroměříž, Czech Republic, August 15-17, 2005. Edited by V. Šimák, M. Šumbera, Š. Todorova, B. Tomášik, AIP Conference Proceedings 828, 2006, ISBN 0-7354-0320-1.

[3] R. Lednický, *ibid* p.423.

[4] M. Lisa, *ibid* p.226.

[5] P. Chaloupka, *ibid* p.610.

[6] M. Bysterský, *ibid* p.205; e-Print Archive: nucl-ex/0511053.

[7] R. Lednický, Proc. CIPQQG'01, Palaiseau, France, arXiv: nucl-th/0112011; Phys. Atom. Nucl. **67**, 72 (2004).

[8] M. Bysterský and F. Retiere: “Measuring scattering length at STAR,” unpublished talk at WPCF 2005. Available at <http://www.particle.cz/conferences/wpcf2005/talks/retiere.ppt>.

[9] Proc. 18th Int. Conf. on Ultra-Relativistic Nucleus-Nucleus Collisions, Budapest, Hungary, 4-9 August, 2005, edited by T. Csörgő, G. Dávid and P. Lévai, Nucl.Phys.A**774** (2006).

[10] R. Lednický, *ibid* 189-198.

[11] P. Chaloupka, *ibid* 603-606.

[12] P. Chaloupka, Proc. SQM 2006 Int. Conf. on Strangeness in quark matter, University of California Los Angeles, 2631 March 2006, edited by Kenneth Barish, Huan Zhong Huang, Joseph Kapusta, Grazyna Odyniec, Johann Rafelski and Charles A Whitten Jr, J. Phys. G: Nucl. Part. Phys. **32** S537-S540 (2006).

[13] J. Adams *et al.* [STAR Collaboration], Nucl. Phys. A **757** (2005) 102.

[14] B. I. Abelev *et al.* [STAR Collaboration], arXiv:nucl-ex/0607012.

[15] J. Adams *et al.* [STAR Collaboration], Phys. Rev. Lett. **95**, 122301 (2005).

[16] D. Molnar and S. A. Voloshin, Phys. Rev. Lett. **91**, 092301 (2003), R. J. Fries, B. Muller, C. Nonaka and S. A. Bass, Phys. Rev. Lett. **90**, 202303 (2003).

[17] J. Adams *et al.* [STAR Collaboration], arXiv:nucl-ex/0606014.

[18] F. Retiere and M. A. Lisa, Phys. Rev. C **70**, 044907 (2004).

[19] R. Lednický, V. L. Lyuboshits, B. Erazmus, and D. Nouais, Phys. Lett. **B373** (1996) 3034.

[20] C. Nonaka and S. A. Bass, Phys. Rev. C **75**, 014902 (2007).

[21] U. W. Heinz, J. Phys. G **31**, S717 (2005).

[22] C. Blume *et al.* [NA49 Collaboration], Nucl. Phys. A **715**, 55 (2003).

[23] J. Adams *et al.* [STAR Collaboration], Phys. Rev. Lett. **91**, 262302 (2003).

[24] P. Chaloupka [STAR Collaboration], Nucl. Phys. A **749**, 283 (2005).

[25] R. Witt, talk at 19th Int. Conf. on Ultra-Relativistic Nucleus–Nucleus Collisions, Shanghai, China, November 14-20, 2006, arXiv:nucl-ex/0701063

[26] J. Adams *et al.* [STAR Collaboration], Phys. Rev. C **71**, 044906 (2005).

[27] Z. Chajecki, T. D. Gutierrez, M. A. Lisa and M. Lopez-Noriega [the STAR Collaboration], arXiv:nucl-ex/0505009.

[28] S. Pratt and S. Petroni, Phys. Rev. C **68**, 054901 (2003).

[29] B. I. Abelev [STAR Collaboration], Phys. Rev. C **74**, 054902 (2006) and S. Bekele, “Neutral Kaon Correlations in 200 GeV/NN Au+Au collisions at RHIC”, proceeding WPCF 2006.

[30] J. Adams *et al.* [STAR Collaboration], arXiv:nucl-ex/0511003.

[31] S. Pislak *et al.* [BNL-E865 Collaboration], Phys. Rev. Lett. **87**, 221801 (2001).

[32] B. Adeva *et al.* [DIRAC Collaboration], Phys. Lett. B **619**, 50 (2005).

[33] D. A. Brown and P. Danielewicz, Phys. Lett. B **398**, 252 (1997).

[34] D. A. Brown and P. Danielewicz, Phys. Rev. C **57**, 2474 (1998).

[35] S. S. Adler *et al.* [PHENIX Collaboration], arXiv:nucl-ex/0605032.

[36] R. Lednický and V.L. Lyuboshitz, Yad. Fiz. **35**, 1316 (1982) [Sov. J. Nucl. Phys. **35**, 770 (1982)]. Fortran program provided by R. Lednický.

[37] M. Csanad, T. Csorgo and M. Nagy, arXiv:hep-ph/0702032.

